Computational and Theoretical Chemistry 1233 (2024) 114485

Contents lists available at ScienceDirect

Computational and Theoretical Chemistry

journal homepage: www.elsevier.com/locate/comptc

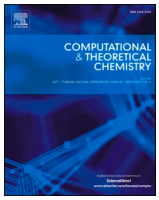

Viewpoint article

A quantum chemical investigation of the interaction of perfluoropropionic acid with monoethanolamine and sulfuric acid in the atmosphere

Flávio Soares Medeiros [a], Kelson M.T. Oliveira [b], Sylvio Canuto [c], Puspitapallab Chaudhuri [a,*]

[a] Department of Materials Physics, Federal University of Amazonas, Manaus, AM, Brazil
[b] Department of Chemistry, Federal University of Amazonas, Manaus, AM, Brazil
[c] Department of General Physics, University of São Paulo, São Paulo, SP, Brazil

ARTICLE INFO

Keywords:
Molecular clusters
Hydrogen bonding
Natural bond orbital (NBO)
Density functional theory (DFT)
Perfluoropropionic acid

ABSTRACT

Perfluoroalkyl substances (PFASs) including Perfluoroalkyl acids (PFAAs), known for their chemical and thermal stability, are widely used in many industrial applications. However, their toxicity and bioaccumulative potential raise environmental and health concerns. PFAAs like Perfluoroalkyl carboxylic acids (PFCAs), detected in atmospheric aerosols, pose risks due to their long-range dispersion. Employing DFT we investigate the interactions of Perfluoropropionic acid (PFPA), a persistent organic pollutant, with atmospheric molecules like Sulfuric acid (SA) and monoethanolamine (MEA). Performing a systematic quantum-chemical analysis on structural and thermochemical properties of various ternary PFPA-SA-MEA clusters, we observe that PFPA forms stable hydrogen-bonded molecular clusters with SA and MEA which may facilitate its propagation in the atmosphere. The presence of both SA and MEA is essential to enhance the interaction capacity of PFPA in ambient condition as indicated by the calculated binding energies. A significant increase in scattering intensities of solar radiation is observed when PFPA forms clusters.

1. Introduction

Theoretical quantum chemistry has evolved into a crucial tool for exploring diverse contemporary molecular phenomena such as the intricate hydrogen-bonding networks of biomolecules within living organisms, complex non-conventional intermolecular interactions in medicinal chemistry, the formation of molecules in the cold interstellar medium, nucleation of aerosol molecules and dispersion of pollutants in the Earth's atmosphere, and many others [1–15]. In the present work we apply quantum-chemical models to analyze the nature of intermolecular interaction of an anthropogenic pollutant called perfluoropropionic acid (PFPA, CF_3CF_2COOH), which is a member of the family of Per- and polyfluorinated alkyl substances (PFASs). This is relevant with respect to its long-range transport in the atmosphere.

The PFASs constitute a diverse group of synthetic organofluorine compounds, all sharing a common feature: a perfluorinated carbon chain of varying lengths. Over the past few decades, PFASs have been extensively employed in the production of a wide array of consumer goods, including food packaging materials, cosmetics, paints, cleaning products, firefighting foams, non-stick cookware, smartphone screens, and stain-resistant textiles [16–30]. Moreover, they play a crucial role in large-scale industrial processes, such as the manufacturing of computer chips, semiconductors, jet engines, automobiles, batteries, medical devices, and refrigeration systems [16–22,31,32]. The exceptional hydrophobic and oleophobic properties of the perfluorinated carbon chain, combined with the remarkable chemical and thermal stability arising from the robust C-F bond, render PFASs highly suitable for these multifaceted applications. However, these compounds are also a cause for concern and classified as persistent organic pollutants (POPs) [33–36] due to their ability to resist degradation, high toxicity, and strong bioaccumulation potential [30,37–44]. Many commonly used PFASs can degrade under oxidative conditions to highly persistent perfluoroalkyl acids (PFAAs) that include perfluoroalkyl carboxylic acids (PFCAs) and perfluoroalkyl sulfonic acids (PFSAs). Studies have shown that PFAAs can be adsorbed onto atmospheric aerosols and transported over long distances, leading to their widespread distribution in the environment [45–51]. In addition, the properties of PFAAs, such as their high boiling points and low vapor pressures, make them more likely to be present in aerosols compared to other chemicals. The presence of PFAAs in atmospheric aerosols has raised concerns about their potential impact on the environment and human health including liver toxicity, developmental and reproductive effects, immune system dysfunction

* Corresponding author.
E-mail address: puspito@ufam.edu.br (P. Chaudhuri).

https://doi.org/10.1016/j.comptc.2024.114485
Received 19 November 2023; Received in revised form 15 January 2024; Accepted 18 January 2024
Available online 24 January 2024
2210-271X/© 2024 Elsevier B.V. All rights reserved.

[40–44,52–66]. When aerosols containing PFAAs are inhaled, they can deposit in the lungs and potentially cause respiratory irritation and other health effects. PFAAs are also found in human blood and breast milk, indicating that people are exposed to these chemicals through various sources [61,67–73]. Additionally, the deposition of PFCAs in natural ecosystems can lead to contamination of soil and water, which can have harmful effects on wildlife [56,63,74–79]. Evaluating the intricate balance between the risks and benefits associated with PFASs and PFAAs is a challenge that demands extensive collaboration among scientists, risk assessors, and regulators. Numerous PFAS-related regulatory initiatives are underway worldwide, focusing on risk assessment, socio-economic analysis, and the quest for PFAS alternatives [80–84]. However, the process of restricting the use of PFAS in industrial settings and reducing their pervasive and enduring presence in various environments must be a time-intensive process. During this period, further research is imperative to gain a deeper understanding of the physicochemical properties of these compounds, their atmospheric presence resulting from both direct and indirect emissions, their environmental transport process, and the associated adverse effects.

Regarding the long-range atmospheric transport of PFAAs and their detection in air, precipitation and aerosol samples in different parts of the world including remote inland environments and sea-spray aerosols [45–51], it is relevant to investigate the intermolecular interactions between PFAA and atmospheric molecules at ambient conditions. Considering this into account, we have performed a detailed quantum-chemical investigation on the behavior of the ternary clusters formed in the atmosphere between perfluoropropionic acid (PFPA, CF_3CF_2COOH), Sulfuric acid (SA, H_2SO_4) and monoethanolamine (MEA, $NH_2CH_2CH_2OH$). PFPA is the simplest member of the perfluoroalkyl carboxylic acid (PFCA, $C_nF_{2n+1}COOH$ with n = 2,3,4 ….) family with a perfluorated C—C bond attached to a carboxyl (COOH) group. In a previous work [85], we observed that PFPA potentially forms strong hydrogen-bonded binary clusters with naturally occurring organic molecules whose strength increases at lower temperatures above the ground-level. H_2SO_4 is considered to be the most significant among the so-called atmospheric nucleation precursors that serve as the initial building blocks for the formation of secondary aerosols [86–90]. These precursors are critical in the process of atmospheric nucleation, where clusters of molecules come together to create tiny particles, which can grow and eventually influence air quality, climate, and cloud formation. MEA, on the other hand, is a primary amine and an organic compound that is commonly used in the chemical industry, where it serves as an important absorbent for the removal of carbon dioxide (CO_2) from industrial gases [91–93]. It is also used in the production of certain surfactants, cosmetics, and pharmaceuticals. While MEA is not as extensively studied as other nucleation precursors like H_2SO_4, recent research has shown that amines, including MEA, can enhance nucleation rates and participate in the growth of molecular clusters in the atmosphere, ultimately leading to the creation of aerosol particles [94–97]. Since the acid-base interactions are found to provide stability to the nucleation process, it may also play relevant role in the formation of PFPA-driven molecular clusters which gets transported to long distances through air. In this article, we consider different possible ternary cluster compositions of PFPA, H_2SO_4 and MEA, namely $(PFPA)(SA)_2$, $(PFPA)(MEA)_2$ and (PFPA)(SA)(MEA) and analyze the structure and thermochemical properties of each cluster composition using density functional theory (DFT) in order to get insight into the nature of intermolecular interactions of PFPA with atmospheric molecules.

2. Computational method

The objective of the present work is to gain insight into the intermolecular interaction pattern and thermodynamical stability of the hydrogen-bonded ternary clusters formed between PFPA, SA and MEA. Since all these molecules can simultaneously donate and accept proton, it is understandable that there should exist several stable conformations of the clusters. So, we conducted a comprehensive search for conformations taking into consideration the potential for proton donation and proton acceptance that may occur during the interactions of these three molecules. Several plausible conformations of ternary clusters formed between PFPA and two SA molecules $(PFPA)(SA)_2$, between PFPA and two MEA molecules, $(PFPA)(MEA)_2$ and between PFPA and one molecules of MEA and H_2SO_4 each (PFPA)(SA)(MEA) were prepared by using Gaussview program [98]. Consequently, geometry optimizations and harmonic frequency calculations were performed for all these clusters using the Gaussian 16 program package [99]. Considering only those having all positive frequencies and structural distinctness, we finally obtained five conformers of $(PFPA)(SA)_2$ clusters, six conformers of $(PFPA)(MEA)_2$ and eight of (PFPA)(SA)(MEA) clusters. Geometry optimizations were performed in two steps – first, with a small basis 6-31++G(d,p) in conjunction with M06-2X [100] and ωB97XD [101,102] functionals and then, with a large 6-311++G(3df, 3pd) basis considering the 6-31++G(d,p) optimized geometries as starting geometry. Thus, the two quantum-chemical models used for final calculations are **Model 1:** M06-2X/6-311++G(3df, 3pd) and **Model 2:** ωB97XD/6-311++G(3df, 3pd). The basis set 6-311++G(3df, 3pd) was chosen as it with M06-2X functional showed excellent performance for estimating cluster formation through binary/ternary nucleation of sulfuric acid and water/ammonia both in neutral and ionized forms [103]. The partial charges were calculated at the same models using natural bond orbital (NBO) method [104–106], as implanted in Gaussian 16.

The binding electronic energies (ΔE) and the binding Gibbs free energies (ΔG) are calculated by subtracting the sum of the constituent monomer energies from the respective cluster energy:

$$\Delta X = X_n(n) - \sum_{i=1}^{n} X_i$$

where $X = E$ (electronic energy) or G (Gibbs free energy), $X_n(n)$ and $X_i$represent the energy of the cluster with n monomers and the energy of the i^{th} isolated monomer, respectively. Corrections for zero-point energy (ZPE) have been considered for both parameters. Since each molecular cluster may possess several energetically stable conformers, the effect of multiple conformers on the cluster binding free energy is calculated as [87,107].

$$\Delta G_{MC} = RT\ln\left[\sum_{k=1}^{n}\exp\left(\frac{-\Delta G_k}{RT}\right)\right].$$

where $R = 8.314\mathrm{J}/(\mathrm{mol}\bullet\mathrm{K})$ is the universal gas constant and T is the ambient temperature.

3. Results and discussions

3.1. Cluster structure analysis

The optimized geometries of the energetically stable conformers of $(PFPA)(SA)_2$, $(PFPA)(MEA)_2$ and (PFPA)(SA)(MEA) ternary clusters, considered in the present work, are shown in Fig. 1, Fig. 2 and Fig. 3, respectively. The equilibrium structure and relevant molecular properties of isolated PFPA had been discussed in our previous paper [85]. As we can see, the cluster geometries are stabilized by the action of different combinations of non-covalent interactions. These interactions include intra-molecular hydrogen bonding (HB), inter-molecular hydrogen bonding between neutral monomers (referred to as neutral HB), and proton-transfer (PT) mediated ionic bonding (referred to as ionic HB). All the three participating monomers – PFPA, SA and MEA – act simultaneously as proton-donor and proton-acceptor forming closed-shaped cyclic molecular clusters in most cases. The structural configurations of the clusters optimized by the two employed models are almost same, with slight variations of the HB parameters among themselves, as reported in the figures. The clusters have been arranged in ascending

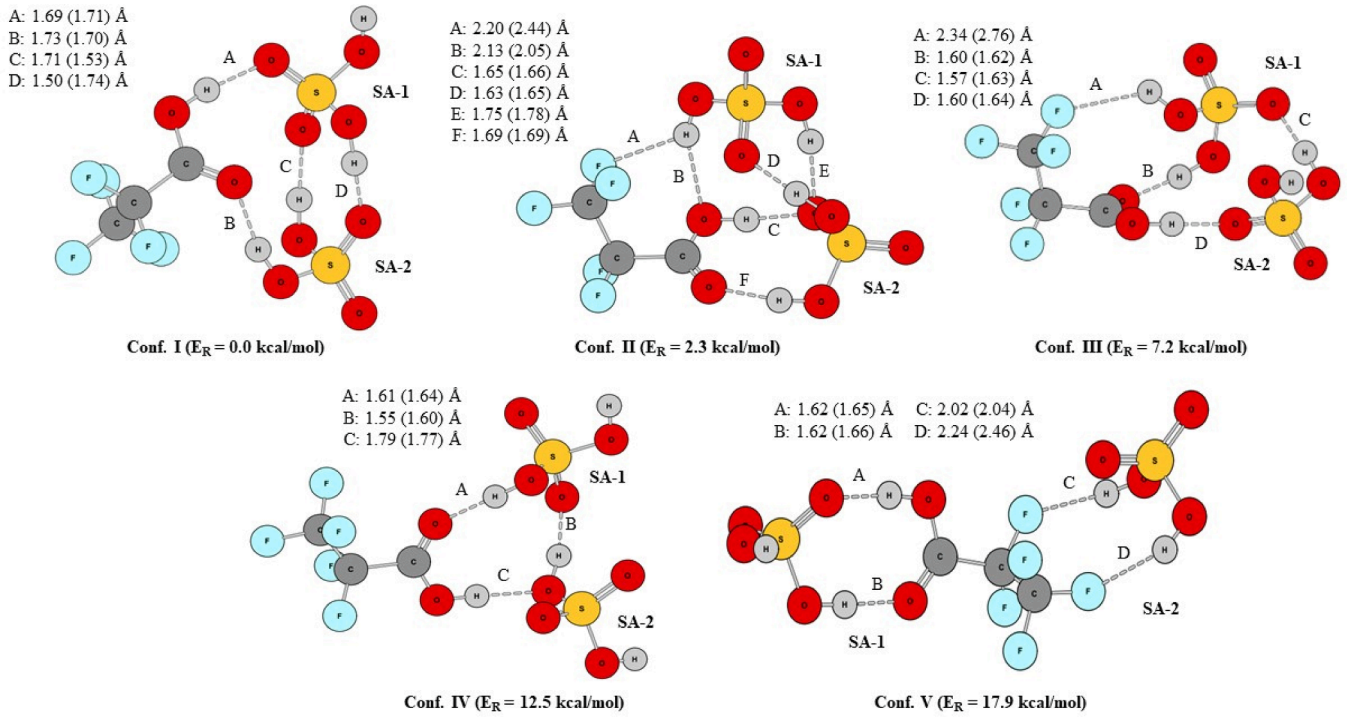

Fig. 1. Optimized structures of the ternary clusters of PFPA with SA considered in the present work. The grey dashed lines labelled by capital letters (A, B, C, etc.) represent the inter-molecular hydrogen bonds. The numbers represent the hydrogen bond lengths as obtained by Model 1 (Model 2).

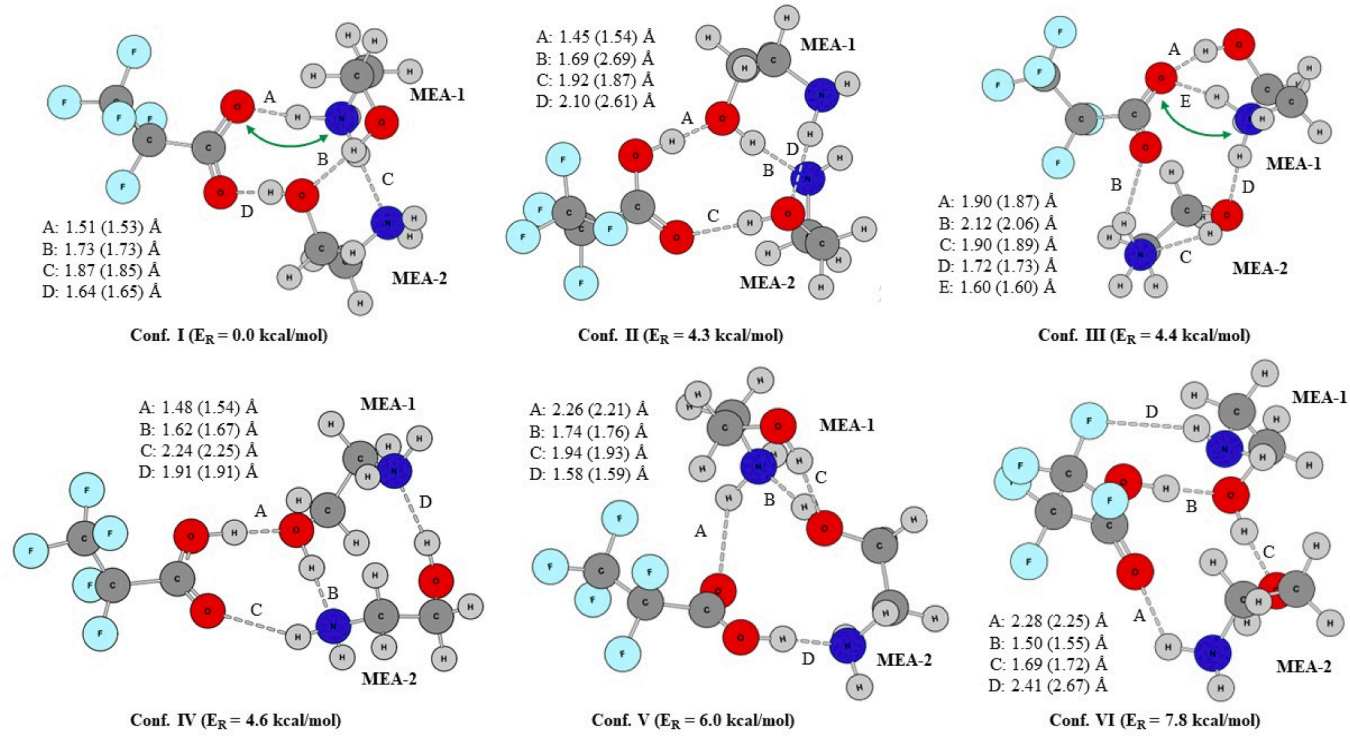

Fig. 2. Optimized structures of the ternary clusters of PFPA with MEA considered in the present work. The grey dashed lines labelled by capital letters (A, B, C, etc.) represent the inter-molecular hydrogen bonds. The numbers represent the hydrogen bond lengths as obtained by Model 1 (Model 2). The green double-sided curved arrow represents the proton transfer site.

order of electronic energy, with the lowest-energy conformer of each cluster species designated as Conf. I. The neutral and ionic HBs present in the clusters are depicted by dashed grey lines and labeled with capital letters A, B, C, and so on. A green double-sided curved arrow is employed to indicate the proton transfer site within a given cluster, as identified by analyses of structural parameters and NBO partial atomic charges. In accordance with the definition outlined in the literature [108], we have considered an occurrence of proton transfer within the

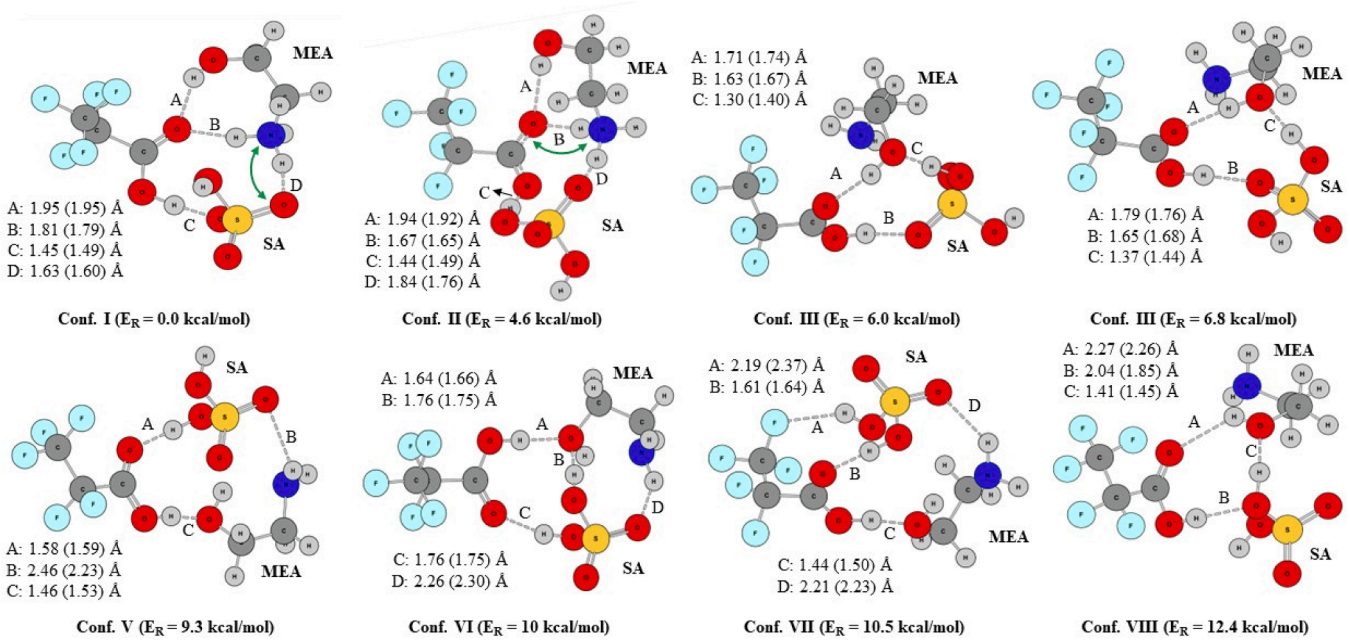

Fig. 3. Optimized structures of the ternary clusters of PFPA with SA and MEA considered in the present work. The grey dashed lines labelled by capital letters (A, B, C, etc.) represent the inter-molecular hydrogen bonds. The numbers represent the hydrogen bond lengths as obtained by Model 1 (Model 2). The green double-sided curved arrow represents the proton transfer site.

cluster when the partial charges of the participating monomers reach a magnitude of at least 0.5*e*. This implies that for proton transfer to occur, there must be a significant difference in partial charge between the donor and acceptor groups involved in the transfer.

(PFPA)(SA)$_2$ clusters: Five conformers of this cluster are identified, all stabilized by the formation of several intermolecular HB between the neutral monomers, as depicted in Fig. 1. The number of HBs formed in each cluster conformer varies from 3 (in Conf. IV) to 5 (Conf. II) and the hydrogen bond lengths (r_{HB}) range from 1.50 (1.53) Å to 2.34 (2.76) Å according to Model 1 (Model 2). The most energetically stable conformer (Conf. I) has four strong O −H···O type HBs as PFPA donates proton to one SA moiety and accepts proton from the other SA moiety, forming two HBs via its COOH group and the two SA moieties form two other HBs among themselves. Similar behavior of PFPA is also observed in Conf. IV. However, a weaker interaction between the two SA moieties makes Conf. IV energetically less stable with a relative energy of +12.5 kcal/mol with respect to Conf. I. The average HB length ($\bar{r}_{HB}$), average O—O distance across the HB ($\bar{R}_{OO}$) and the average bond angle ($\bar{\theta}_{HB}$) in Conf. I, as determined by Model I, are 1.66 Å, 2.64 Å and 171°, respectively. These values closely adhere to the criteria for a hydrogen bond of moderate strength, as defined in the literature [1]. In Conf. II, the corresponding parameters are as follows: $\bar{r}_{HB} = 1.77$ Å, $\bar{R}_{OO} = 2.73$ Å and $\bar{\theta}_{O-H\cdots O} = 165°$. These values also fall into the category of moderate HBs. However, when compared to Conf. I, both $\bar{r}_{HB}$ and $\bar{R}_{OO}$ in Conf. II are longer, while $\bar{\theta}_{O-H\cdots O}$ is smaller. These differences likely account for Conf. II being 2.3 kcal/mol less stable than Conf. I despite having a higher number of HBs. In none of these conformers the fluorine (F) atoms of PFPA takes part in hydrogen bonding interactions. Among the five conformers, only in Conf. III and V we observe direct participation of fluorine forming O—H···F type HBs, where the C—F bonds acts as proton acceptor. However, the O—H···F bond lengths are fairly high compared to the average O—H···O bond length (1.67 Å) and as a consequence, O—H···F bond strength should be weaker. Thus, despite being the most electronegative atom, hydrogen bonds with fluorine atom do not contribute significantly to the stability of the clusters. This is consistent with the literature showing that organic fluorine is weak hydrogen-bond acceptor [109,110]. The Conf. V of (PFPA)(SA)2, which is the least energetically stable conformer among those considered, is the only one that possesses two O—H···F hydrogen bonds (HBs). This is facilitated by the placement of two SA moieties at opposite ends of PFPA, thus minimizing steric hindrances to the fluorine atoms. This is the only conformer that does not have a cyclic structure.

No proton transfer was observed in any of the (PFPA)(SA)$_2$ conformers by structural and charge analyses which is expected as proton transfer occurs mainly in acid-base interaction. The NBO partial charges of the monomers are also well below the magnitude of 0.5*e*, as can be seen from Table 1.

(PFPA)(MEA)$_2$ clusters: The nature of intermolecular interactions in the ternary clusters formed between PFPA and two MEA molecules, (PFPA)(MEA)$_2$ are slightly different from those of (PFPA)(SA)$_2$. Among the six conformations of (PFPA)(MEA)$_2$ considered in this work, two (Conf. I and III) indicate occurrence of proton transfer between PFPA and one of the MEA moieties, forming (PFP A^-)(MEA^+)(MEA) clusters and $N - H^+\cdots O^-$ type ionic HB, which is well supported by NBO partial charge calculations. In both of these conformers, the large distance between the oxygen and hydrogen atoms of the COOH of PFPA (labelled by the letter A in respective figures) clearly shows that a complete charge separation of the OH bond has occurred while cluster formation. Thus in these two cases we have interactions between PFP A^- or $CF_3CF_2COO^-$ and MEA^+ or $OHCH_2CH_2NH_3^+$. The proton-transfer sites are indicated by

Table 1
Calculated values of NBO partial charges associated with different conformers of (PFPA)(SA)$_2$ ternary clusters as obtained by **Model 1:** M06-2X/6-311++G(3df, 3pd) and **Model 2:** ωB97XD/6-311++G(3df, 3pd).

Systems	Model	PFPA	SA-1	SA-2
(PFPA)(SA)$_2$	1	−0.008*e*	−0.016*e*	0.024*e*
Conf. I	2	−0.001*e*	0.008*e*	0.005*e*
(PFPA)(SA)$_2$	1	0.005*e*	−0.013*e*	0.008*e*
Conf. II	2	0.007*e*	0.007*e*	−0.014*e*
(PFPA)(SA)$_2$	1	0.012*e*	−0.012*e*	0
Conf. III	2	0.0155*e*	−0.0063*e*	−0.0092*e*
(PFPA)(SA)$_2$	1	0.024*e*	−0.041*e*	0.018*e*
Conf. IV	2	0.018*e*	0.008*e*	−0.026*e*
(PFPA)(SA)$_2$	1	0.016*e*	−0.007*e*	−0.009*e*
Conf. V	2	0.012*e*	−0.008*e*	−0.004*e*

a green double-headed curved arrow. As can be seen from Table 2, the partial charges on PFPA and MEA-1 are −0.81*e* (−0.82*e*) and 0.78e (0.78e), respectively at Model 1 (Model 2) in the most stable conformation (Conf. I) of (PFPA)$(MEA)_2$ which are significantly higher than 0.5e. In case of Conf. III, the partial charges on the same moieties are even slightly higher.

From the structural point of view, Conf. I – the most stable conformer of (PFPA)$(MEA)_2$ – is stabilized by the formation of four intermolecular noncovalent bonds – one proton-transfer mediated $N-H^+\cdots O^-$ ionic bond as discussed above, two O −H···O type neutral HBs where the MEAs are the proton-donor and one N −H···N type HB formed between two MEA moieties. On the other hand, Conf. III has higher numbers of non-covalent interactions including one proton-transfer mediated $N-H^+\cdots O^-$ ionic HB between PFPA and MEA-1 like Conf. I and one strong intra-molecular HB of ca. 1.9 Å in MEA-2. However, the oxygen of PFPA that loses proton to NH_2 of MEA-1, simultaneously accepts proton from the OH group of same MEA-1, which may effectively diminish the strength of the ionic bonding to certain extent and may explain the reason behind Conf. III having higher electronic energy compared to Conf. I. The Conf. III is the only one among all the (PFPA)$(MEA)_2$, clusters considered where an intra-molecular HB is observed. In all other conformers of (PFPA)$(MEA)_2$, four neutral HBs are also detected. Among these bonds where OH of PFPA acts as proton-donor, forming O −H···O/N type hydrogen bond, there is a considerable OH bond stretching, ranging from 0.063 to 0.075 Å.

Considering further the two $N-H^+\cdots O^-$ ionic HBs present in Conf. I and Conf. III, we observe that the interatomic distance between the nitrogen and oxygen is same in both conformers which is ca. 2.6 Å, but the distance between H^+ and O^- is 1.5 Å in Conf. I while it is 1.6 Å in Conf. III, at both models. On the other hand, comparing the structural parameters of the neutral HBs in Conf. I and Conf. III, we observe that the average bond length of the neutral HBs ($\bar{r}_{HB}$) is longer, and the average bond angle ($\bar{\theta}_{HB}$) is smaller in Conf. II. For example, while in Conf. I, $\bar{r}_{HB} = 1.75$ Å and $\bar{\theta}_{HB} \approx 170°$, in Conf. II, $\bar{r}_{HB} = 1.91$ Å and $\bar{\theta}_{HB} \approx 153°$, representing weaker hydrogen bonding interaction. The Conf. I has two O—H···O and one N—H···N type HBs, Conf. III has two N—H···O and one O—H···O type hydrogen bonds. Thus, individually the ionic HB in Conf. III might be stronger than Conf. I, but the combined strength of the neutral HBs in Conf. I may be higher that of Conf III. This might be another reason for the higher electronic energy of Conf. III compared to Conf. I.

The relative energies of conf. II, III and IV with respect to Conf. I are practically the same that lie within 4.4–4.6 kcal/mol, although their structural characteristics are significantly different. In both Conf. II and IV, the PFPA moiety, via its OH group, donates proton to OH of MEA-1 (labelled by the letter A in the figure) which in turn acts as proton donor to NH_2 of MEA-2 (labelled by B) and thus forming a sequence of one O −H···O and one O −H···N type HB. The main difference between these conformers lies in the different relative positions of MEA-1 with respect to MEA-2, that allows MEA-2 to form a N −H···O HB with PFPA in Conf. IV, and a O −H···O HB with PFPA in Conf. II, with PFPA being the proton acceptor in both cases. These interactions are identified by the letter C in the figure. Moreover, a fourth HB is formed in both conformers (labelled by D) as in Conf. II the MEA-1 moiety forms a N −H···O HB donating proton to the OH of MEA-2 via its NH_2 group, while in Conf. IV, it uses the same NH_2 group to accept proton from OH of MEA-2 and forms a O −H···N HB. The O −H···N bond length is slightly shorter than the N −H···O bond. Conf. VI is the only geometry of (PFPA)$(MEA)_2$ that possesses N −H···F type HB, which again falls into the category of weak HB with $r_{HB}(H\cdots F) = 2.41$ (2.67) Å and $R_{NF} = 3.13$ (3.40) Å at Model 1 (Model 2) and should not contribute effectively to the energetic stability.

(PFPA)(SA)(MEA) clusters: Eight different conformations of 1:1:1 ternary clusters formed by PFPA, SA and MEA are considered. The two lowest energy conformations (Conf. I and II), demonstrate proton transfer between acid and base moieties. In Conf. I, one of the O—H groups of SA loses proton to NH_2 of MEA, forming a (PFPA)$(SA^-)(MEA^+)$ cluster, while in Conf. II, the proton transfer occurs between the COOH group of PFPA and NH_2 of MEA forming a $(PFPA^-)(SA)(MEA^+)$ cluster. The $N-H^+\cdots O^-$ ionic HB lengths and bond angles are 1.63 (1.60) Å and 163° (174°) in Conf. I and 1.60 (1.65) Å and 160° (174°) in Conf. II at Model 1 (Model2). NBO analysis shows that the electronic charge fractions on SA and MEA in Conf. I are −0.800*e* and +0.870*e*, respectively, while the same for PFPA and MEA in Conf. II are −0.795*e* and +0.880*e*, as par Model 1, corroborating with observation that strong proton transfer effect is present in these conformers. Calculations with Model 2 show similar results, as can be seen from Table 3.

Apart from the ionic HBs, both Conf. I and Conf. II feature three neutral HBs, of which one is of the O −H···N type and other two are of the O −H···O type. In fact, all conformers exhibit two or more O −H···O type neutral HBs and in all cases, except the Conf. VI, one of them is notably a very strong HB featuring a super-stretched O—H bond ($R_{OH} >$ 1.0 Å), while the other bonds are moderate or weak in strength. The average value of the O—H bond stretch (ΔR_{OH}) of these strong O −H···O HBs (labelled always by the letter C in Fig. 3) is ca. 0.077 Å, with Conf. III having the highest stretch ($\Delta R_{OH} = 0.14$ Å). The average O — O distance (R_{OO}) across the HB and the average bond angle (∠O −H···O) are 2.45 Å and 174°, respectively which align closely with the criteria for a strong hydrogen bond as defined in the literature [86]. To give specific examples, we may state that $R_{OO} = 2.49$ (2.42) Å and ∠O −H···O = 174° (178°), in Conf. I (Conf. III). The Conf. VI is the only conformer where all of its three neutral O −H···O type HBs are of moderate strength, as par literature [97], with average $R_{OO} = 2.68$ Å and average ∠O −H···O = 165°. Conf. VIII, the (PFPA)(SA)(MEA) cluster

Table 2
Calculated values of NBO partial charges associated with different conformers (PFPA)$(MEA)_2$ ternary clusters as obtained by **Model 1:** M06-2X/6-311++G (3df, 3pd) and **Model 2:** ωB97XD/6-311++G(3df, 3pd).

Systems	Model	PFPA	MEA-1	MEA-2
(PFPA)$(MEA)_2$ Conf. I	1	−0.814*e*	0.778*e*	0.035*e*
	2	−0.817*e*	0.777*e*	0.040*e*
(PFPA)$(MEA)_2$ Conf. II	1	−0.084*e*	0.006*e*	0.078*e*
	2	−0.068*e*	0.051*e*	0.017*e*
(PFPA)$(MEA)_2$ Conf. III	1	−0.8714*e*	0.8315*e*	0.0399*e*
	2	−0.864*e*	0.823*e*	0.041*e*
(PFPA)$(MEA)_2$ Conf. IV	1	−0,091*e*	0.027*e*	0.064*e*
	2	−0.076*e*	0.026*e*	0.050*e*
(PFPA)$(MEA)_2$ Conf. V	1	−0.111*e*	0.061*e*	0.050*e*
	2	−0.109*e*	0.062*e*	0.047*e*
(PFPA)$(MEA)_2$ Conf. VI	1	−0.093*e*	0.053*e*	0.040*e*
	2	−0.081*e*	0.041*e*	0.040*e*

Table 3
Calculated values of NBO partial charges associated with different conformers (PFPA)(MA)(MEA) ternary clusters as obtained by **Model 1:** M06-2X/6-311++G(3df, 3pd) and **Model 2:** ωB97XD/6-311++G(3df, 3pd).

Systems	Model	PFPA	S.A.	M.E.A
(PFPA)(SA)(MEA) Conf. I	1	−0.065*e*	−0.800*e*	0.870*e*
	2	−0.044*e*	−0.819*e*	0.863*e*
(PFPA)(SA)(MEA) Conf. II	1	−0.795*e*	−0.085*e*	0.880*e*
	2	−0.802*e*	−0.058*e*	0.860*e*
(PFPA)(SA)(MEA) Conf. III	1	−0.006*e*	−0.123*e*	0.129*e*
	2	−0.005*e*	−0.093*e*	0.099*e*
(PFPA)(SA)(MEA) Conf. IV	1	−0.0192*e*	−0.0933*e*	0.1125*e*
	2	−0.009*e*	−0.078*e*	0.087*e*
(PFPA)(SA)(MEA) Conf. V	1	−0.038*e*	−0.060*e*	0.098*e*
	2	−0.020*e*	−0.060*e*	0.080*e*
(PFPA)(SA)(MEA) Conf. VI	1	−0.024*e*	−0.057*e*	0.081*e*
	2	−0.018*e*	−0.068*e*	0.086*e*
(PFPA)(SA)(MEA) Conf. VII	1	−0.045*e*	−0.055*e*	0.100*e*
	2	−0.038*e*	−0.048*e*	0.086*e*
(PFPA)(SA)(MEA) Conf. VIII	1	−0.010*e*	−0.113*e*	0.123*e*
	2	−0.020*e*	−0.090*e*	0.110*e*

with highest energy with a large energy difference of 12.4 kcal/mol from global minimum, also contains three neutral O −H···O type HBs in the equilibrium structure. Among these HBs, the one labeled as C represents strong interaction with R_{OO} = 2.49 Å and ∠O −H···O = 178°. On the other hand, the other two bonds (labeled as A and B) are typical example of weak hydrogen bonding with R_{OO} = 2.49 (2.42) Å and ∠O −H···O = 178° (178°) for bond A (bond B). These weaker interactions may contribute to the relatively lower energetic stability of this cluster. Furthermore, Conf. VII is the only cluster that features a weak C −F···H −O HB, formed between PFPA and SA, with R_{OF} = 2.99 Å and ∠O −H···F = 140° and no OH stretch. Additionally, Conf. V, VI and VII possess one N −H···O = S type neutral HB formed between MEA and SA with N −H of MEA being the proton donor, but all these bonds are weak with R_{ON} = 3.00 Å (in all three cluster) and ∠N −H···O = 121° (Conf. V), 127° (Conf. VI) and 134° (Conf. VII). All numerical values mentioned in this section were obtained by using Model 1: M06-2X/6-311++G (3df,3pd). The Model 2: ωB97XD/6-311++G(3df,3pd) provides very similar results. The partial NBO charges on PFPA, SA and MEA moieties of Conf. III to Conf. VIII are all quite smaller than 0.5*e* supporting the conclusion that no proton transfer has occurred in these clusters.

3.2. Thermodynamic stability and equilibrium constant analysis

In Table 4, we present the calculated binding electronic energy (Δ*E*) and the binding Gibbs free energy of formation (Δ*G*), both corrected for the zero-point energy. Additionally, we include the values of equilibrium constant (K_{eq}) corresponding to each cluster, all calculates at 298.15 K using both levels of calculations. The K_{eq} values were calculated by using the formula: $K_{eq} = e^{-\Delta G/RT}$ where R = 8.314J/(mol • K) is the universal gas constant and T = 298.15 K is the ambient temperature.

Table 4
Calculated values of binding electronic energies (Δ*E*), binding free energy (Δ*G*), in kcal/mol, and the equilibrium constants (K_{eq}) at 298.15 K, for different ternary clusters formed by PFPA with SA and MEA as obtained by - **Model 1:** M06-2X/6-311++G(3df, 3pd) and **Model 2:** ωB97XD/6-311++G(3df, 3pd).

Systems	Model	Δ*E*	Δ*G*	K_{eq}
$(PFPA)(MEA)_2$ Conf. I	1	−31.14	−8.99	4.0×10^6
	2	−33.44	−10.67	6.8×10^7
$(PFPA)(MEA)_2$ Conf. II	1	−26.85	−3.99	8.5×10^2
	2	−23.92	−1.64	1.6×10^1
$(PFPA)(MEA)_2$ Conf. III	1	−25.86	−2.26	4.5
	2	−27.72	−4.31	1.5×10^3
$(PFPA)(MEA)_2$ Conf. IV	1	−26.81	−4.84	3.6×10^3
	2	−27.21	−5.00	4.6×10^3
$(PFPA)(MEA)_2$ Conf. V	1	−25.45	−2.84	1.2×10^2
	2	−25.51	−2.23	4.3×10^1
$(PFPA)(MEA)_2$ Conf. VI	1	−23.73	−0.08	1.1
	2	−22.96	0.89	2.2×10^{-1}
$(PFPA)(SA)_2$ Conf. I	1	−35.76	−12.16	8.4×10^8
	2	−35.35	−9.98	2.1×10^7
$(PFPA)(SA)_2$ Conf. II	1	−32.71	−8.23	1.1×10^6
	2	−33.05	−7.19	1.9×10^5
$(PFPA)(SA)_2$ Conf. III	1	−28.70	−5.67	1.4×10^4
	2	−29.23	−5.19	6.4×10^3
$(PFPA)(SA)_2$ Conf. IV	1	−23.21	−0.18	1.4
	2	−24.02	−0.42	2.0
$(PFPA)(SA)_2$ (Conf. V)	1	−17.85	4.12	9.5×10^{-4}
	2	−18.89	3.40	3.2×10^{-3}
(PFPA)(MEA)(SA) Conf. I	1	−37.82	−14.28	3.1×10^{10}
	2	−40.73	−18.22	2.4×10^{13}
(PFPA)(MEA)(SA) Conf. II	1	−33.52	−10.38	4.1×10^7
	2	−35.63	−12.53	1.5×10^9
(PFPA)(MEA)(SA) Conf. III	1	−33.74	−9.64	1.2×10^7
	2	−32.15	−7.50	3.2×10^5
(PFPA)(MEA)(SA) Conf. IV	1	−32.47	−8.78	2.8×10^6
	2	−32.05	−8.00	7.4×10^5
(PFPA)(MEA)(SA) Conf. V	1	−29.29	−5.76	1.7×10^4
	2	−29.58	−5.43	9.7×10^3
(PFPA)(MEA)(SA) Conf. VI	1	−28.12	−5.33	8.1×10^3
	2	−29.05	−5.73	1.6×10^4
(PFPA)(MEA)(SA) Conf. VII	1	−28.58	−4.92	4.1×10^3
	2	−28.73	−5.26	7.2×10^3
(PFPA)(MEA)(SA) Conf. VIII	1	−26.39	−2.06	3.2×10^1
	2	−25.36	−1.75	1.9×10^1

As we can observe, all the clusters exhibit negative and expressively high value of Δ*E* in both models, and most of them also demonstrate negative Δ*G* that would represent greater stability of the cluster compared to the corresponding monomers at ambient temperature. In fact, among the five $(PFPA)(SA)_2$ and six $(PFPA)(MEA)_2$ conformers considered here, only the highest energy conformer in each case shows thermodynamic instability. All the eight (PFPA)(MEA)(SA) conformers show negative Δ*G* at ambient temperature at both models. The calculated values of ΔE show certain model dependencies, with Δ*E* (Model 2) being slightly lower than Δ*E* (Model 1) in most cases where the differences between the two models vary between 0.5 and 7.5 %. Maximum difference is observed in Conf. II of $(PFPA)(MEA)_2$ where Δ*E* (Model 2) is higher than Δ*E* (Model 1) by ca. 11 %, which is an exception as in all other clusters the variations are restricted within 7.7 %. The calculated values of Δ*G* also show similar model dependencies, although Model 2 shows lower values in higher number of cases. Among the three cluster compositions, (PFPA)(MEA)(SA) has the highest thermodynamical stability with the lowest value of Δ*G* which is –14.3 (–18.2) kcal/mol obtained Model 1 (Model 2).

The differences between the Δ*G* values of the local minima and that of the global minimum of each cluster composition is quite appreciable. Consequently, Conf. I of each cluster composition is the major contributor when the effect of multiple conformers on the cluster binding free energy is calculated, or in other words, $\Delta G_{MC} = \Delta G$(Conf. I) in all three cluster compositions – $(PFPA)(SA)_2$, $(PFPA)(MEA)_2$ and (PFPA)(MEA)(SA). The equilibrium constant of a chemical system is a measure of the proportion of products and reactants present at a given equilibrium state. In the context of the formation of atmospheric particle cluster, the magnitude of the equilibrium constant is directly related to the extent of Gibb's free energy change. A lower variation of the free energy corresponds to a higher equilibrium constant, indicating a greater concentration of clusters formed in the atmosphere. Therefore, a high equilibrium constant signifies that cluster formation is favored over dissociation. In each cluster composition considered here – $(PFPA)(SA)_2$, $(PFPA)(MEA)_2$ and (PFPA)(MEA)(SA) – the free energy variations of the local minima are significantly greater than that of the global minimum (Conf. I). As a result, Conf. I consistently exhibits a much higher equilibrium constant value, indicating that this specific configuration is more energetically favored over others. Furthermore, upon comparing the global minimum of each composition, the following order is observed: K_{eq}[(PFPA)(MEA)(SA)] ≈ 10^{10} > K_{eq}[$(PFPA)(SA)_2$] ≈ 10^9 > K_{eq}[$(PFPA)(MEA)_2$] ≈ 10^6 as determined by Model 1. This implies that, under ambient conditions, the relative population of Conf. I of (PFPA)(MEA)(SA) cluster will be approximately 10,000 times greater than that of Conf. I of $(PFPA)(MEA)_2$, and approximately 10 times more than that of Conf. I of $(PFPA)(SA)_2$, confirming that interaction with an acid-base combination is important for PFPA's effective participation in cluster formation.

It is well-known that in the troposphere, the lowest layer of Earth's atmosphere, temperature generally decreases with an increase in altitude. Considering this fact, we have performed thermochemical calculations for each ternary cluster at three different temperatures − 298 K, 244 K and 217 K. The variations of Δ*G* with temperature for the clusters, as obtained by Model 1, are demonstrated in Fig. 4. All clusters, including Conf. VI of $(PFPA)(SA)_2$ that has positive Δ*G* at 298 K, show large increase in thermodynamical stability as temperature decreases.

3.3. Interaction with solar radiation

In the field of aerosol science, the elastic and inelastic scattering of

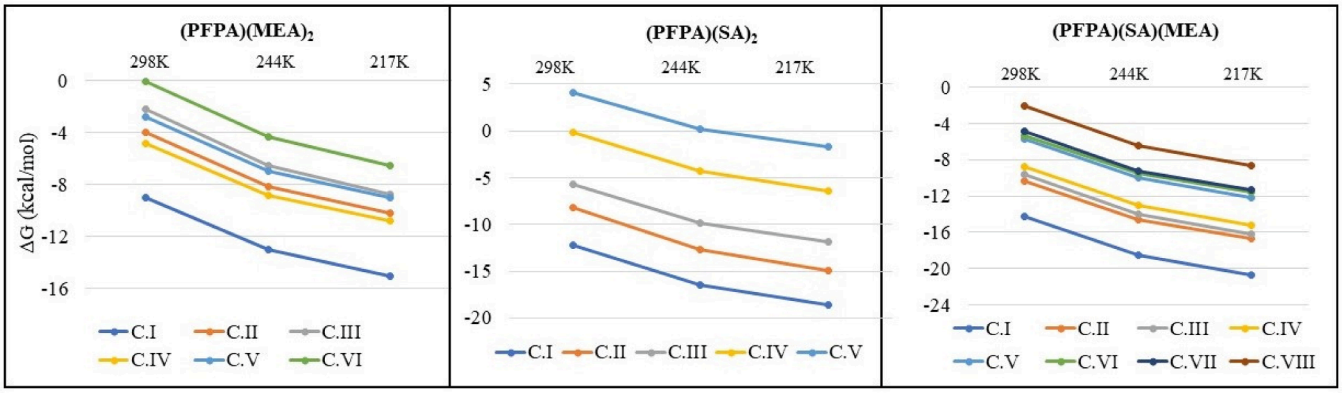

Fig. 4. Temperature dependence of the binding free energy ΔG (kcal/mol) of the ternary cluster conformers of PFPA with SA and MEA obtained by Model 1.

solar radiation by atmospheric particles plays a significant role in understanding various phenomena related to visibility and radiative forcing in the atmosphere. Rayleigh scattering or elastic scattering of light, in particular, is the predominant optical event for small atmospheric molecular clusters, and it is responsible for several atmospheric processes. The intensity of Rayleigh scattering, also known as Rayleigh activity, is influenced by the dipole polarizability and the anisotropy of the polarizability of the molecular systems. Isotropic dipole polarizability represents the ability of a molecule to respond to an electric field and is related to the magnitude of the induced dipole moment in response to the electric field. Anisotropy of the polarizability refers to the directional dependence of the polarizability. These properties determine how strongly the incident radiation interacts with the molecules and the subsequent scattering intensity. In Table 5 we report the dipole moments (μ), isotropic dipole polarizability ($\overline{\alpha}$) and anisotropy of the polarizability ($\Delta\alpha$) of all the clusters along with the corresponding the Rayleigh Activity ($\Re$) and degree of depolarization (σ) for natural light calculated by using the formulas [111–114].

$$\Re_n = 45(\overline{\alpha})^2 + 13(\Delta\alpha)^2$$

and

$$\sigma_n = \frac{6(\Delta\alpha)^2}{45(\overline{\alpha})^2 + 7(\Delta\alpha)^2},$$

with the subscript n representing natural light.

As can be seen from Table 5, the dipole moments calculated by the two models are quite similar in most cases, with Conf. I of $(PFPA)(MEA)_2$ having the highest dipole moment ($\mu \approx 9$ Debye) among all cluster compositions. The dipole moments, however, vary appreciably among the conformers of each cluster composition. For example, among the (PFPA)(MEA)(SA) conformers, Conf. VI has the highest dipole moment at both models ($\mu \approx 7$ Debye) while Conf. IV possesses the lowest dipole moment with $\mu \approx 3$ Debye. In case of $(PFPA)(MEA)_2$, while Conf. I has the highest dipole moment with $\mu \approx 7$ Debye, Conf. VI has the lowest dipole moment with $\mu \approx 4$ Debye. The isotropic polarizabilities ($\overline{\alpha}$), on the other hand, do not show such variations and within each cluster composition, the individual values of $\overline{\alpha}$of the conformers lie very close to the respective average value ($\langle\overline{\alpha}\rangle$) as evidenced by the respective Relative Standard Deviations (RSD). The RSD ($\overline{\alpha}$) for $(PFPA)(SA)_2$, $(PFPA)(MEA)_2$ and (PFPA)(MEA)(SA), as obtained by Model 1, are just 0.53 %, 0.95 % and 0.65 %, respectively. Considering the values of $\langle\overline{\alpha}\rangle$ as obtained by Model 1, we can arrange the cluster compositions in order of increasing polarizability as follows: $(PFPA)(SA)_2$ [$\langle\overline{\alpha}\rangle$= 116.1 a. u.] < (PFPA)(MEA)(SA) [$\langle\overline{\alpha}\rangle$= 121.7 a. u.] < (PFPA)(MEA)2 [$\langle\overline{\alpha}\rangle$= 129.3 a. u.].

Performing the same analysis with anisotropy of the polarizability ($\Delta\alpha$), we observe a different order of increasing anisotropy: $(PFPA)(MEA)_2$ [$\langle\Delta\alpha\rangle = 26.2$ a. u.] < (PFPA)(MEA)(SA) [$\langle\Delta\alpha\rangle = 28.3$ a. u.] < $(PFPA)(SA)_2$ [$\langle\Delta\alpha\rangle = 30.9$ a. u.], where $\langle\Delta\alpha\rangle$ is the average of the $\Delta\alpha$ values of the cluster conformers. Thus, among the three cluster compositions considered here, although $(PFPA)(MEA)_2$ exhibits the highest polarizability and consequently the largest molecular volume, it is the least anisotropic among them. The (PFPA)(MEA)(SA) composition falls in between $(PFPA)(MEA)_2$ and $(PFPA)(SA)_2$ in terms of both polarizability and anisotropy. The RSD($\Delta\alpha$) for $(PFPA)(SA)_2$, $(PFPA)(MEA)_2$,

Table 5
Calculated values of dipole moment (μ) in Debye (D), mean dipole polarizabilty ($\overline{\alpha}$), polarizability anisotropy ($\Delta\alpha$), degree of depolarization (σ_n) and Rayleigh activity for natural light ($\Re_n$) in a.u. of different stable PFPA ternary clusters as obtained by **Model 1:** M06-2X/6-311++G(3df, 3pd) and **Model 2:** ωB97XD/6-311++G(3df, 3pd).

Systems	Model	μ	$\overline{\alpha}$	Δα	σ_n	$\Re_n$
$(PFPA)(MEA)_2$ Conf. I	1	8.63	129.6	26.45	0.0055	764,741
	2	9.09	131.9	25.27	0.0049	790,910
$(PFPA)(MEA)_2$ Conf. II	1	5.12	130.1	25.99	0.0053	769,861
	2	5.16	131.9	28.30	0.0061	792,780
$(PFPA)(MEA)_2$ Conf. III	1	6.29	127.2	22.97	0.0043	735,437
	2	6.71	130.0	22.97	0.0041	767,521
$(PFPA)(MEA)_2$ Conf. IV	1	4.67	129.9	31.79	0.0079	772,978
	2	4.27	132.5	31.28	0.0074	803,176
$(PFPA)(MEA)_2$ Conf. V	1	5.53	128.9	26.32	0.0055	756,092
	2	5.88	131.4	26.58	0.0054	786,454
$(PFPA)(MEA)_2$ Conf. VI	1	4.39	127.6	22.03	0.0040	739,011
	2	4.38	130.3	21.40	0.0036	769,371
$(PFPA)(SA)_2$ Conf. I	1	5.67	115.9	32.08	0.0101	617,671
	2	5.97	119.1	32.85	0.0100	651,821
$(PFPA)(SA)_2$ Conf. II	1	3.88	115.3	30.89	0.0095	610,103
	2	3.94	118.0	30.72	0.0089	639,029
$(PFPA)(SA)_2$ Conf. III	1	3.39	116.1	28.04	0.0077	616,996
	2	3.46	118.9	28.15	0.0074	646,504
$(PFPA)(SA)_2$ Conf. IV	1	2.98	116.0	27.79	0.0076	615,417
	2	2.86	118.8	27.48	0.0071	645,295
$(PFPA)(SA)_2$ Conf. V	1	5.13	117.0	37.68	0.0136	634,762
	2	5.34	19.6	36.87	0.0125	660,805
(PFPA)(MEA)(SA) Conf. I	1	7.11	121.9	27.94	0.0069	678,459
	2	5.54	125.9	32.70	0.0089	726,734
(PFPA)(MEA)(SA) Conf. II	1	6.48	122.2	28.59	0.0072	682,868
	2	6.99	125.6	30.49	0.0078	722,398
(PFPA)(MEA)(SA) Conf. III	1	3.49	121.1	25.51	0.0059	668,731
	2	3.56	123.9	24.39	0.0051	698,209
(PFPA)(MEA)(SA) Conf. IV	1	2.96	121.5	24.07	0.0052	672,177
	2	2.66	124.5	24.41	0.0051	705,414
(PFPA)(MEA)(SA) Conf. V	1	3.72	121.9	34.05	0.0103	683,152
	2	4.27	125.1	32.06	0.0087	717,196
(PFPA)(MEA)(SA) Conf. VI	1	7.33	122.1	30.84	0.0084	684,201
	2	7.53	124.7	31.00	0.0082	712,037
(PFPA)(MEA)(SA) Conf. VII	1	4.69	121.1	30.04	0.0081	671,840
	2	4.65	124.0	29.77	0.0076	702,942
(PFPA)(MEA)(SA) Conf. VIII	1	4.14	119.8	23.70	0.0052	653,257
	2	4.21	123.2	25.60	0.0057	691,747

and (PFPA)(MEA)(SA) obtained from Model 1 are 12.8 %, 13.1 %, and 12.6 % respectively, indicating that the anisotropy values of the conformers within each cluster composition exhibit considerable variation around the mean compared to the isotropic polarizability. Model 2 provides similar trends in the results. When considering the individual Δα values of the conformers within each cluster composition, we observe that among the $(PFPA)(MEA)_2$ conformers, Conf. IV exhibits the highest anisotropy. Similarly, among the $(PFPA)(SA)_2$ and (PFPA)(MEA)(SA) conformers, Conf. V in both cluster compositions demonstrate the highest level of anisotropy.

Both Rayleigh activity and degree of depolarization depend on mean isotropic polarizability ($\overline{\alpha}$)and anisotropy (Δα) of the system. However, $\overline{\alpha}$ being the major contributor in Rayleigh activity, the large variations of Δα around the mean value in each cluster composition do not affect the $\Re_n$ values. On the other hand, the variations of σ_n follow the same pattern of that of Δα – higher the anisotropy, higher is the degree of depolarization. Thus, the Rayleigh activities of the individual conformers in all the cluster compositions remain close to the respective average value of Rayleigh activities ($\langle\Re_n\rangle$) As par Model 1, RSD ($\Re_n$) for $(PFPA)(SA)_2$, $(PFPA)(MEA)_2$ and (PFPA)(MEA)(SA) are 2.1 %, 2.6 % and 1.5 %, respectively. In order of increasing $\langle\Re_n\rangle$ at ambient condition the cluster compositions can be arranged as follows: $(PFPA)(SA)_2 <$ (PFPA)(MEA)(SA) $<$ $(PFPA)(MEA)_2$. Thus, $(PFPA)(MEA)_2$ shows highest Rayleigh scattering intensity which is ca. 23 % (22 %) higher than that of $(PFPA)(SA)_2$ and 13 % (11 %) higher than that of (PFPA)(MEA)(SA) according to Model 1 (Model 2). In case of isolated PFPA, the values $\Re_n$are calculated as 98,766 and 104,908 a. u. at Model 1 [M06-2X/**6-3**11++G(3df, 3pd)] and Model 2 [ωB97-XD/**6-3**11++G(3df, 3pd)], respectively. Comparing the values of $\Re_n$(PFPA) with those of the clusters, we observe that $(PFPA)(MEA)_2$ suffers maximum variation upon cluster formation, with $\frac{\langle\Re_n\rangle[(PFPA)(MEA)_2]}{\Re_n(PFPA)} \approx 8$, followed by (PFPA)(MEA)(SA) with $\frac{\langle\Re_n\rangle[(PFPA)(MEA)(SA)]}{\Re_n(PFPA)} \approx 7$, and $(PFPA)(SA)_2$ with $\frac{\langle\Re_n\rangle[(PFPA)(SA)_2]}{\Re_n(PFPA)} \approx 6$. The increase of Rayleigh activity in $(PFPA)(SA)_2$ cluster with respect to isolated PFPA is less than other organic acids including sulfuric acid itself forming cluster with sulfuric acid dimer, $(SA)_2$ For example, in a previous study[34] with M062X/aug-cc-pVTZ, it was found that when H_2SO_4 trimer or $(SA)_3$ is formed, $\langle\Re_n\rangle$ increases by ca. 9 times compared to $\Re_n$(SA) and in $(MSA)(SA)_2$, $\langle\Re_n\rangle$ increases by ca. 7 times compared to $\Re_n$(MSA) where MSA stands for Methanesulfonic Acid. As far as the degree of depolarization for natural light (σ_n) is concerned, it is highest in $(MSA)(SA)_2$ followed by (PFPA)(MEA)(SA) and $(PFPA)(MEA)_2$, following the same trend of anisotropy. The average degree of depolarization, $\langle\sigma_n\rangle$ of the three cluster compositions are 0.0095 (0.0089) a. u., 0.0071 (0.0077) a. u. and 0.0054 (0.0052) a. u. for $(MSA)(SA)_2$, (PFPA)(MEA)(SA) and $(PFPA)(MEA)_2$, respectively at Model1 (Model 2).

4. Conclusion

Studying the formation of hydrogen-bonded molecular clusters in the Earth's atmosphere hold significant implications for comprehending atmospheric chemistry and addressing air pollution. This study focuses on exploring the structure and thermochemical properties of some ternary clusters formed by Perfluoropropionic acid (PFPA) with sulfuric acid (SA) and monoethanolamine (MEA). PFPA belongs to the group of persistent organic pollutants (POPs) that have a long environmental lifespan and are known to have adverse effects on human health. Three different cluster compositions, namely $(PFPA)(SA)_2$, $(PFPA)(MEA)_2$ and (PFPA)(MEA)(SA) and several energetically stable conformers of each composition are investigated by two Density Functional-based models: M062X/6-311++G(3df,3pd) and ωB97XD/6-311++G(3df,3pd), at ambient temperature. The optimized geometries of cluster conformers are stabilized by different combinations of non-covalent interactions, including intra- and intermolecular hydrogen bonding and proton transfer. All three participating monomers simultaneously act as proton donors and acceptors, forming closed cyclic molecular clusters in most cases. The most energetically stable conformer of $(PFPA)(MEA)_2$ as well as that of (PFPA)(MEA)(SA) clusters exhibit proton transfer between PFPA and MEA, leading to ionic hydrogen-bond interactions. The hydrogen bond strengths in $(PFPA)(MEA)_2$ clusters are weaker compared to other two compositions, resulting in lowest thermodynamic stability with multiple-conformer binding free energy, $\Delta G_{MC} = -9.0$ kcal/mol at the M062X/6-311++G(3df,3pd) level of calculation. In contrast, the ΔG_{MC}values of $(PFPA)(SA)_2$ and (PFPA)(MEA)(SA) are −12.2 kcal/mol and −14.3 kcal/mol, respectively, at the same level of calculation. With ωB97XD/6-311++G(3df,3pd) the values are −10,7 kcal/mol, −10,0 kcal/mol and −18,2kcal/mol, for $(PFPA)(MEA)_2$, $(PFPA)(SA)_2$ and (PFPA)(MEA)(SA), respectively. Thus, the presence of acid-base combination (SA and MEA) is found to be essential for PFPA to form more thermodynamically stable clusters in the atmosphere. Additionally, the most stable conformer (Conf. I) of each cluster composition exhibits predominant relative populations, with high equilibrium constants. These global conformers are energetically favored and represent the majority of the cluster populations. With lowering of temperature, thermodynamic stability increases for all clusters. Furthermore, the interaction of the clusters with solar radiation, specifically Rayleigh scattering, is studied. Rayleigh activity depends on the isotropic dipole polarizability and anisotropy of polarizability of the molecular systems, with the former being the dominant contributor. Comparing the Rayleigh activity values of the clusters with that of the PFPA monomer, it is observed that cluster formation causes significant increase in the Rayleigh intensity, with the largest variation observed in the $(PFPA)(MEA)_2$ cluster. The results obtained provide insights into the behavior of the pollutant molecule PFPA regarding its interactions with important atmospheric molecules under standard atmospheric conditions.

CRediT authorship contribution statement

Flávio Soares Medeiros: Visualization, Investigation, Formal analysis, Data curation. **Kelson M.T. Oliveira:** Writing – review & editing, Formal analysis. **Sylvio Canuto:** Writing – review & editing, Formal analysis. **Puspitapallab Chaudhuri:** Writing – original draft, Supervision, Resources, Project administration, Methodology, Investigation, Formal analysis, Conceptualization.

Declaration of competing interest

The authors declare that they have no known competing financial interests or personal relationships that could have appeared to influence the work reported in this paper.

Data availability

Data will be made available on request.

Acknowledgments

The authors acknowledge financial support from the Brazilian funding agencies CAPES (Coordenação de Aperfeiçoamento de Pessoal de Nível Superior) – finance code 001, FAPEAM (Fundação de Amparo à Pesquisa do Estado do Amazonas) – POSGRAD, CNPq (Conselho Nacional de Desenvolvimento Científico e Tecnológico) and the National Institute of Science and Technology Complex Fluids (INCT-FCx), the São Paulo Research Foundation (FAPESP – 2014/50983-3).

References

[1] G.A. Jeffrey, An Introduction to Hydrogen Bonding, Oxford University Press, 1997.
[2] S. Scheiner, Hydrogen Bonding: A Theoretical Perspective, Oxford University Press, New York, 1997.

[3] C.L. Perrin, J.B. Nielson, "Strong" hydrogen bonds in chemistry and biology, Annu. Rev. Phys. Chem. 48 (1997) 511–544, https://doi.org/10.1146/annurev.physchem.48.1.511.

[4] L.J. Karas, C.-H. Wu, R. Das, J.-I.-C. Wu, Hydrogen bond design principles, WIREs Comput. Mol. Sci. 10 (2020) e1477, https://doi.org/10.1002/wcms.1477.

[5] E. Arunan, G.R. Desiraju, R.A. Klein, J. Sadlej, S. Scheiner, I. Alkorta, D.C. Clary, R.H. Crabtree, J.J. Dannenberg, P. Hobza, H.G. Kjaergaard, A.C. Legon, B. Mennucci, D.J. Nesbitt, Definition of the hydrogen bond (IUPAC Recommendations 2011), Pure Appl. Chem. 83 (2011) (2011) 1637–1641, https://doi.org/10.1351/PAC-REC-10-01-02.

[6] Y. Lin, Y. Ji, Y. Li, J. Secrest, W. Xu, F. Xu, Y. Wang, T. An, R. Zhang, Interaction between succinic acid and sulfuric acid–base clusters, Atmos. Chem. Phys. 19 (2019) 8003–8019, https://doi.org/10.5194/acp-19-8003-2019.

[7] J. Elm, D. Ayoubi, M. Engsvang, A.B. Jensen, Y. Knattrup, J. Kubečka, C. J. Bready, V.R. Fowler, S.E. Harold, O.M. Longsworth, G.C. Shields, Quantum chemical modeling of organic enhanced atmospheric nucleation: a critical review, WIREs Comput. Mol. Sci. 13 (2023) e1662, https://doi.org/10.1002/wcms.1662.

[8] J.L. Jeffrey, J.A. Terrett, D.W. MacMillan, O-H hydrogen bonding promotes H-atom transfer from α C-H bonds for C-alkylation of alcohols, Science 349 (2015) 1532–1536, https://doi.org/10.1126/science.aac8555.

[9] H. Wang, X. Wang, Y. Hu, Z. Su, X. Zhang, Q. Zhang, M.H. Hadizadeh, X. Zhao, F. Xu, Y. Sun, W. Wang, The effect of water molecules and air humidity on the cluster formation from benzoic acid with sulfuric acid/ammonia/dimethylamine: a molecular-scale investigation, J. Mol. Liq. 390 (2023) 123001, https://doi.org/10.1016/j.molliq.2023.123001.

[10] E.E. Etim, P. Gorai, A. Das, S.K. Chakrabarti, E. Arunan, Interstellar hydrogen bonding, Adv. Space Res. 61 (2018) 2870–2880, https://doi.org/10.1016/j.asr.2018.03.003.

[11] G. Bovolenta, S. Bovino, E. Vöhringer-Martinez, D.A. Saez, T. Grassi, S. Vogt-Geisse, High level ab initio binding energy distribution of molecules on interstellar ices: hydrogen fluoride, Mol. Astrophys. 21 (2020) 100095, https://doi.org/10.1016/j.molap.2020.100095.

[12] B. Kuhn, P. Mohr, M. Stahl, Intramolecular hydrogen bonding in medicinal chemistry, J. Med. Chem. 53 (2010) 2601–2611, https://doi.org/10.1021/jm100087s.

[13] Z. Osifová, O. Socha, L. Mužíková Čechová, M. Šála, Z. Janeba, M. Dračínský, Eur. J. Org. Chem. (2021) 4166–4173, https://doi.org/10.1002/ejoc.202100721.

[14] C. Zuo, X. Zhao, H. Wang, X. Ma, S. Zheng, F. Xu, Q. Zhang, A theoretical study of hydrogen-bonded molecular clusters of sulfuric acid and organic acids with amides, J. Environ. Sci. 100 (2021) 328–339, https://doi.org/10.1016/j.jes.2020.07.022.

[15] Y. Maréchal, From physics to biology: a journey through science accompanying the hydrogen bond and the water molecule, J. Mol. Struct. 880 (2008) 38–43, https://doi.org/10.1016/j.molstruc. 2007.12.041.

[16] L.G.T. Gaines, Historical and current usage of per- and polyfluoroalkyl substances (PFAS): a literature review, Am. J. Ind. Med. 66 (2023) 353–378, https://doi.org/10.1002/ajim.23362.

[17] F.G. Torres, G.E. De-la-Torre, Per- and polyfluoroalkyl substances (PFASs) in consumable species and food products, J. Food Sci. Technol. 60 (2023) 2319–2336, https://doi.org/10.1007/s13197-022-05545-7.

[18] Environment Agency, Poly- and perfluoroalkyl substances (PFAS): sources, pathways and environmental data, Environment Agency, Bristol, 2021, https://www.gov.uk/government/publications/poly-and-perfluoroalkyl-substances-pfas-sources-pathways-and-environmental-data (accessed October 21, 2023).

[19] M.G. Evich, M.J.B. Davis, J.P. McCord, B. Acrey, J.A. Awkerman, D.R.U. Knappe, A.B. Lindstrom, T.F. Speth, C. Tebes-Stevens, M.J. Strynar, Z. Wang, E.J. Weber, W. Matthew Henderson, J.W. Washington, Per- and polyfluoroalkyl substances in the environment, Science 375 (2022) eabg9065, https://doi.org/10.1126/science.abg9065.

[20] J. Glüge, R. London, I.T. Cousins, J. DeWitt, G. Goldenman, D. Herzke, R. Lohmann, M. Miller, C.A. Ng, S. Patton, X. Trier, Z. Wang, M. Scheringer, Information requirements under the essential-use concept: PFAS case studies, Environ. Sci. Technol. 56 (2022) 6232–6242, https://doi.org/10.1021/acs.est.1c03732.

[21] B. Cheng, K. Alapaty, V. Zartarian, A. Poulakos, M. Strynar, T. Buckle, Per- and polyfluoroalkyl substances exposure science: current knowledge, information needs, future directions, Int. J. Environ. Sci. Technol. 19 (2022) 10393–10408, https://doi.org/10.1007/s13762-021-03710-7.

[22] K.J. Harris, Occurrence of Per-and Polyfluoroalkyl substances in Cosmetics and Personal Care Products, Carleton University, Ottawa, Ontario, 2022. Master's thesis.

[23] J. Glüge, M. Scheringer, I.T. Cousins, J.C. DeWitt, G. Goldenman, D. Herzke, R. Lohmann, C.A. Ng, X. Trierm, Z. Wang, An overview of the uses of per- and polyfluoroalkyl substances (PFAS), Environ. Sci. Process Impacts 22 (2020) 2345–2373, https://doi.org/10.1039/d0em00291g.

[24] C.A. Moody, J.A. Field, Perfluorinated surfactants and the environmental implications of their use in fire-fighting foams, Environ. Sci. Technol. 34 (2000) 3864–3870, https://doi.org/10.1021/es991359u.

[25] A.K. Tokranov, N. Nishizawa, C.A. Amadei, J.E. Zenobio, H.M. Pickard, J. G. Allen, C.D. Vecitis, E.M. Sunderland, How do we measure poly- and perfluoroalkyl substances (PFASs) at the surface of consumer products? Environ. Sci. Technol. Lett. 6 (2019) 38–43, https://doi.org/10.1021/acs.estlett.8b00600.

[26] Z. Wang, J.C. DeWitt, C.P. Higgins, I.T. Cousins, A Never-ending story of per- and polyfluoroalkyl substances (PFASs)? Environ. Sci. Technol. 51 (2017) 2508–2518, https://doi.org/10.1021/acs.est.6b04806.

[27] M. Kotthoff, J. Müller, H. Jürling, M. Schlummer, D. Fiedler, Perfluoroalkyl and polyfluoroalkyl substances in consumer products, Environ. Sci. Pollut. Res. 22 (2015) 14546–14559, https://doi.org/10.1007/s11356-015-4202-7.

[28] Y. Fujii, K.H. Harada, A. Koizumi, Occurrence of perfluorinated carboxylic acids (PFCAs) in personal care products and compounding agents, Chemosphere 93 (2013) 538–544.

[29] D. Herzke, E. Olsson, S. Posner, Perfluoroalkyl and polyfluoroalkyl substances (PFASs) in consumer products in Norway: a pilot study, Chemosphere 88 (2012) 980–987, https://doi.org/10.1016/j.chemosphere.2012.03.03.

[30] R.C. Buck, J. Franklin, U. Berger, J.M. Conder, I.T. Cousins, P. de Voogt, A. A. Jensen, K. Kannan, S.A. Mabury, S.P.J. van Leeuwen, Perfluoroalkyl and polyfluoroalkyl substances in the environment: terminology, classification, and origins, Integr. Environ. Assess. Manage. 7 (2011) 513–541, https://doi.org/10.1002/ieam.258.

[31] X. Lim, Could the world go PFAS-free? Proposal to ban 'forever chemicals' fuels debate, Nature 620 (2023) 24–27, https://doi.org/10.1038/d41586-023-02444-5.

[32] B. Tansel, PFAS use in electronic products and exposure risks during handling and processing of e-waste: a review, J. Environ. Manag. 316 (2022) 115291, https://doi.org/10.1016/j.jenvman.2022.115291.

[33] K.C. Jones, Persistent organic pollutants (POPs) and related chemicals in the global environment: some personal reflections, Environ. Sci. Technol. 55 (2021) 9400–9412, https://doi.org/10.1021/acs.est.0c08093.

[34] K.C. Jones, P. Voogt, Persistent organic pollutants (POPs): state of the science, Environ. Pollut. 100 (1999) 209–221, https://doi.org/10.1016/S0269-7491(99)00098-6.

[35] T. Groffen, J. Rijnders, L. van Doorn, C. Jorissen, S. Mortier De Borger, D. O. Luttikhuis, L. de Deyn, A. Covaci, L. Bervoets, Preliminary study on the distribution of metals and persistent organic pollutants (POPs), including perfluoroalkylated acids (PFAS), in the aquatic environment near Morogoro, Tanzania, and the potential health risks for humans, Environ. Res. 192 (2021) 110299, https://doi.org/10.1016/j.envres.2020.110299.

[36] N. Ghosh, S. Roy, J.A. Mondal, On the behavior of perfluorinated persistent organic pollutants (POPs) at environmentally relevant aqueous interfaces: an interplay of hydrophobicity and hydrogen bonding, Langmuir 36 (2020) 3720–3729, https://doi.org/10.1021/acs.langmuir.0c00189.

[37] H.-T. Do, L.-A. Phan Thi, N.H. Dao Nguyen, C.-W. Huang, Q.V. Le, V.-H. Nguyen, Tailoring photocatalysts and elucidating mechanisms of photocatalytic degradation of perfluorocarboxylic acids (PFCAs) in water: a comparative overview, J. Chem. Technol. Biotechnol. 95 (2020) 2569–2578, https://doi.org/10.1002/jctb.6333.

[38] J.M. Conder, R.A. Hoke, W. Wolf, M.H. Russell, R.C. Buck, Are PFCAs bioaccumulative? A critical review and comparison with regulatory criteria and persistent lipophilic compounds, Environ. Sci. Technol. 42 (2008) 995–1003, https://doi.org/10.1021/es070895g.

[39] H. Brunn, G. Arnold, W. Körner, G. Rippen, K.G. Steinhäuser, I. Valentin, PFAS: forever chemicals-persistent, bioaccumulative and mobile. Reviewing the status and the need for their phase out and remediation of contaminated sites, Environ. Sci. Eur. 35 (2023) 20, https://doi.org/10.1186/s12302-023-00721-8.

[40] J.E. Zenobio, O.A. Salawu, Z. Han, A.S. Adeley, Adsorption of per- and polyfluoroalkyl substances (PFAS) to containers, J. Hazard. Mater. Adv. 7 (2022) 100130, https://doi.org/10.1016/j.hazadv.2022.100130.

[41] L. Ahrens, J. Hedlund, W. Dürig, R. Tröger, K. Wiberg, Screening of PFASs in Groundwater and Surface Water, Institutionen för vatten och miljö, Uppsala, Sweden, 2016.

[42] K. Steenland, T. Fletcher, C.R. Stein, S.M. Bartell, L. Darrow, M.J.L. Espinosa, P. B. Ryan, D.A. Savitz, Review: Evolution of evidence on PFOA and health following the assessments of the C8 science panel, Environ. Int. 145 (2020) 106125, https://doi.org/10.1016/j.envint.2020.106125.

[43] Z. Wang, I.T. Cousins, M. Scheringer, K. Hungerbuehler, Hazard assessment of fluorinated alternatives to long-chain perfluoroalkyl acids (PFAAs) and their precursors: status quo, ongoing challenges and possible solutions, Environ. Int. 75 (2015) 172–179, https://doi.org/10.1016/j.envint.2014.11.013.

[44] I.T. Cousins, J.C. Dewitt, J. Gluge, G. Goldenman, D. Herzke, et al., The high persistence of PFAS is sufficient for their management as a chemical class, Environ. Sci.: Processes Impacts 22 (2020) 2307–2312, https://doi.org/10.1039/D0EM00355G.

[45] J.H. Johansson, M.E. Salter, J.C. Acosta Navarro, C. Leck, E.D. Nilsson, I. T. Cousins, Global transport of perfluoroalkyl acids via sea spray aerosol, Environ. Sci.: Processes Impacts 21 (2019) 635–649, https://doi.org/10.1039/c8em00525g.

[46] A. Dreyer, V. Matthias, C. Temme, R. Ebinghaus, Annual time series of air concentrations of polyfluorinated compounds, Environ. Sci. Technol. 43 (2009) 4029–4036, https://doi.org/10.1021/es900257w.

[47] C.E. Müller, A.C. Gerecke, C. Bogdal, Z. Wang, M. Scheringer, K. Hungerbühler, Atmospheric fate of poly- and per fluorinated alkyl substances (PFASs): I. Day–night patterns of air concentrations in summer in Zurich, Switzerland, Environ. Pollut. 169 (2012) 196–203, https://doi.org/10.1016/j.envpol.2012.04.010.

[48] J.P. Benskin, V. Phillips, V.L. St. Louis, J.W. Martin, Source elucidation of perfluorinated carboxylic acids in remote alpine lake sediment cores, Environ. Sci. Technol. 45 (2011) 7188–7194, https://doi.org/10.1021/es2011176.

[49] W. Liu, J. Wu, W. He, F. Xu, A review on perfluoroalkyl acids studies: environmental behaviors, toxic effects, and ecological and health risks, Ecosyst. Health Sustain. 5 (2019) 1–19, https://doi.org/10.1080/20964129.2018.1558031.

[50] J.A. Faust, PFAS on atmospheric aerosol particles: a review, Environ. Sci. Processes Impacts 25 (2023) 133–150, https://doi.org/10.1039/D2EM00002D.

[51] H.P.H. Arp, K.-U. Goss, Gas/particle partitioning behavior of perfluorocarboxylic acids with terrestrial aerosols, Environ. Sci. Technol. 43 (2009) 8542–8547, https://doi.org/10.1021/es901864s.

[52] C.A. McDonough, W. Li, H.N. Bischel, A.O. de Silva, J.C. DeWitt, Widening the lens on PFASs: direct human exposure to perfluoroalkyl acid precursors (pre-PFAAs), Environ. Sci. Technol. 56 (2022) 6004–6013, https://doi.org/10.1021/acs.est.2c00254.

[53] A.A. Aquilina-Beck, J.L. Reiner, K.W. Chung, M.J. DeLise, P.B. Key, M. E. DeLorenzo, Uptake and biological effects of perfluorooctane sulfonate exposure in the adult eastern oyster *Crassostrea virginica*, Arch. Environ. Contam. Toxicol. 79 (2020) 333–342, https://doi.org/10.1007/s00244-020-00765-4.

[54] K. Winkens, G. Giovanoulis, J. Koponen, R. Vestergren, U. Berger, A.M. Karvonen, J. Pekkanen, H. Kiviranta, I.T. Cousins, Perfluoroalkyl acids and their precursors in floor dust of children's bedrooms–Implications for indoor exposure, Environ. Int. 119 (2018) 493–502, https://doi.org/10.1016/j.envint.2018.06.009.

[55] M.E. Morales-McDevitt, J. Becanova, A. Blum, T.A. Bruton, S. Vojta, M. Woodward, R. Lohmann, The air that we breathe: neutral and volatile PFAS in indoor air, Environ. Sci. Technol. Lett. 8 (2021) 897–902, https://doi.org/10.1021/acs.estlett.1c00481.

[56] J. Wu, M. Junaid, Z. Wang, W. Sun, N. Xu, Spatiotemporal distribution, sources and ecological risks of perfluorinated compounds (PFCs) in the Guanlan River from the rapidly urbanizing areas of Shenzhen, China, Chemosphere 245 (2020) 125637, https://doi.org/10.1016/j.chemosphere.2019.125637.

[57] C. Gao, Z. Hua, X. Li, Distribution, sources, and dietetic-related health risk assessment of perfluoroalkyl acids (PFAAs) in the agricultural environment of an industrial-agricultural interaction region (IAIR), Changshu, East China, Sci. Total Environ. 809 (2022) 152159, https://doi.org/10.1016/j.scitotenv.2021.152159.

[58] I.T. Cousins, G. Goldenman, D. Herzke, R. Lohmann, M. Miller, et al., The concept of essential use for determining when uses of PFASs can be phased out, Environ. Sci. Technol. 53 (2019) 9964–9967, https://doi.org/10.1039/c9em00163h.

[59] E. Costello, S. Rock, N. Stratakis, S.P. Eckel, D.I. Walker, Exposure to per- and polyfluoroalkyl substances and markers of liver injury: a systematic review and meta-analysis, Environ. Health Perspect. 130 (2022) 046001, https://doi.org/10.1289/ehp10092.

[60] C. Beans, How "forever chemicals" might impair the immune system, PNAS 118 (2021) e2105018118, https://doi.org/10.1073/pnas.2105018118.

[61] A.O. de Silva, PFAS exposure pathways for humans and wildlife: a synthesis of current knowledge and key gaps in understanding, Environ. Toxicol. Chem. 40 (2021) 631–657, https://doi.org/10.1002/etc.4935.

[62] X. Chen, et al., Direct contact membrane distillation for effective concentration of perfluoroalkyl substances – impact of surface fouling and material stability, Water Res. 182 (2020) 116010, https://doi.org/10.1016/j.watres.2020.116010.

[63] L. Ahrens, M. Bundschuh, Fate and effects of poly- and perfluoroalkyl substances in the aquatic environment: a review, Environ. Toxicol. Chem. 33 (2014) 1921–1929, https://doi.org/10.1002/etc.2663.

[64] S. Rayne, K. Forest, Perfluoroalkyl sulfonic and carboxylic acids: a critical review of physicochemical properties, levels and patterns in waters and wastewaters, and treatment methods, J. Environ. Sci. Health A 44 (2009) 1145–1149, https://doi.org/10.1080/10934520903139811.

[65] Z. Ren, U. Bergmann, T. Leiviskä, Reductive degradation of perfluorooctanoic acid in complex water matrices by using the UV/sulfite process, Water Res. 205 (2021) 117676, https://doi.org/10.1016/j.watres.2021.117676.

[66] M. Altarawneh, A closer look into the contribution of atmospheric gas-phase pathways in the formation of perfluorocarboxylic acids, Atmos. Pollut. Res. 12 (2021) 101255, https://doi.org/10.1016/j.apr.2021.101255.

[67] H.F. Hassan, H. Bou Ghanem, J. Abi Kharma, M.G. Abiad, J. Elaridi, M. Bassil, Perfluorooctanoic acid and perfluorooctane sulfonate in human milk: first survey from Lebanon, Int. J. Environ. Res. Public Health 20 (2023) 821, https://doi.org/10.3390/ijerph20010821.

[68] J.S. LaKind, J. Naiman, M.A. Verner, L. Lévêque, S. Fenton, Per- and polyfluoroalkyl substances (PFAS) in breast milk and infant formula: a global issue, Environ. Res. 219 (2023) 115042, https://doi.org/10.1016/j.envres.2022.115042.

[69] H. Kang, K. Choi, H.S. Lee, D.H. Kim, N.Y. Park, Elevated levels of short carbon-chain PFCAs in breast milk among Korean women: current status and potential challenges, Environ. Res. 148 (2016) 351–359, https://doi.org/10.1016/j.envres.2016.04.017.

[70] M.K. So, N. Yamashita, S. Taniyasu, Q. Jiang, J.P. Giesy, K. Chen, L.K.S. Lam, Health risks in infants associated with exposure to perfluorinated compounds in human breast milk from Zhoushan, China, Environ. Sci. Technol. 40 (2006) 2924–2929, https://doi.org/10.1021/es060031f.

[71] B. Göckener, T. Weber, H. Rüdel, M. Bücking, M. Kolossa-Gehring, Human biomonitoring of per- and polyfluoroalkyl substances in German blood plasma samples from 1982 to 2019, Environ. Int. 145 (2020) 106123, https://doi.org/10.1016/j.envint.2020.106123.

[72] H. Nilsson, et al., Inhalation exposure to fluorotelomer alcohols yield perfluorocarboxylates in human blood? Environ. Sci. Technol. 44 (2010) 7717–7722, https://doi.org/10.1021/es101951t.

[73] G. Zheng, E. Schreder, J.C. Dempsey, N. Uding, V. Chu, G. Andres, S. Sathyanarayana, A. Salamova, Per- and polyfluoroalkyl substances (PFAS) in breast milk: concerning trends for current-use PFAS, Environ. Sci. Technol. 55 (11) (2021) 7510–7520, https://doi.org/10.1021/acs.est.0c06978.

[74] H.A. Kaboré, S. Vo, G. Munoz, L. Méité, M. Desrosiers, J. Liu, T. Karim, S. Sauvé, Worldwide drinking water occurrence and levels of newly-identified perfluoroalkyl and polyfluoroalkyl substances, Sci. Total Environ. 616–617 (2018) 1089–1100, https://doi.org/10.1016/j.scitotenv.2017.10.210.

[75] A.J. Lewis, X. Yun, D.E. Spooner, M.J. Kurz, E.R. McKenz, C.M. Sales, Exposure pathways and bioaccumulation of per-and polyfluoroalkyl substances in freshwater aquatic ecosystems: key considerations, Sci. Total Environ. 822 (2022) 153561, https://doi.org/10.1016/j.scitotenv.2022.153561.

[76] L. Mark, R. Brusseau, H. Anderson, B. Guo, PFAS Concentrations in soils: background levels versus contaminated sites, Sci. Total Environ. 740 (2020) 140017, https://doi.org/10.1016/j.scitotenv.2020.140017.

[77] R. Mahinroosta, L. Senevirathna, A review of the emerging treatment technologies for PFAS contaminated soils, J. Environ. Manage. 255 (2020) 109896, https://doi.org/10.1016/j.jenvman.2019.109896.

[78] H.N.P. Vo, et al., Poly-and perfluoroalkyl substances in water and wastewater: a comprehensive review from sources to remediation, J. Water Process Eng. 36 (2020) 101393, https://doi.org/10.1016/j.jwpe.2020.101393.

[79] T.G. Ambaye, M. Vaccari, S. Prasad, et al., Recent progress and challenges on the removal of per- and poly-fluoroalkyl substances (PFAS) from contaminated soil and water, Environ. Sci. Pollut. Res. 29 (2022) 58405–58428, https://doi.org/10.1007/s11356-022-21788-5.

[80] T. Thomas, A. Malek, J. Arokianathar, E. Haddad, J. Matthew, Global regulations around PFAS: the past, the present and the future, Int. Chem. Regul. Law Rev. 6 (2023) 3–17.

[81] N.M. Brennan, A.T. Evans, M.K. Fritz, S.A. Peak, H.E. von Holst, Trends in the regulation of per- and polyfluoroalkyl substances (PFAS): a scoping review, Int. J. Environ. Res. Public Health 18 (2021) 10900, https://doi.org/10.3390/ijerph182010900.

[82] S. Brendel, É. Fetter, C. Staude, L. Vierke, A. Biegel-Engler, Short-chain perfuoroalkyl acids: environmental concerns and a regulatory strategy under REACH, Environ. Sci. Eur. 30 (2018) 1–11, https://doi.org/10.1186/s12302-018-0134-4.

[83] UNEP (United Nations Environment Programme), Conference of the Parties to the Stockholm Convention on Persistent Organic Pollutants. Decision SC-9/4: Perfluorooctane sulfonic acid, its salts and perfluorooctane sulfonyl fluoride, UNEP, Geneva, Switzerland, 2019, doi: 10.1016/j.chemosphere.2022.137549.

[84] USEPA (United States Environmental Protection Agency) EPA PFAS action plan: program update, 2020, https://www.epa.gov/sites/production/files/2020-01/documents/pfas_action_plan_feb2020.pdf (accessed October 21, 2023).

[85] F.S. Medeiros Jr, C. Mota, P. Chaudhuri, Perfluoropropionic acid-driven nucleation of atmospheric molecules under ambient conditions, Chem. A Eur. J. 126 (2022) 8449–8458, https://doi.org/10.1021/acs.jpca.2c05068.

[86] M. Xiao, C.R. Hoyle, L. Dada, D. Stolzenburg, A. Kürten, M. Wang, et al., The driving factors of new particle formation and growth in the polluted boundary layer, Atmos. Chem. Phys. 21 (2021) 14275–14291, https://doi.org/10.5194/acp-21-14275-2021.

[87] J. Elm, J. Kubečka, V. Besel, M.J. Jääskeläinen, R. Halonen, T. Kurtén, H. Vehkamäki, Modeling the formation and growth of atmospheric molecular clusters: a review, J. Aerosol Sci. 149 (2020) 105621, https://doi.org/10.1016/j.jaerosci.2020.105621.

[88] S.-H. Lee, H. Gordon, H. Yu, K. Lehtipalo, R. Haley, Y. Li, R. Zhang, New particle formation in the atmosphere: from molecular clusters to global climate, J. Geophys. Res.: Atmosp. 124 (2019) 7098–7146, https://doi.org/10.1029/2018JD029356.

[89] B. Temelso, T.E. Morrell, R.M. Shields, M.A. Allodi, E.K. Wood, K.N. Kirschner, T. C. Castonguay, K.A. Archer, G.C. Shields, Quantum mechanical study of sulfuric acid hydration: atmospheric implications, J. Phys. Chem. A 116 (2012) 2209–2224, https://doi.org/10.1021/jp2119026.

[90] M. Sipila, T. Berndt, T. Petaja, D. Brus, J. Vanhanen, F. Stratmann, J. Patokoski, R.L. Mauldin, A.-P. Hyvarinen, H. Lihavainen, et al., The role of sulfuric acid in atmospheric nucleation, Science 327 (2010) 1243–1246, https://doi.org/10.1126/science.1180315.

[91] P. Luis, Use of monoethanolamine (MEA) for CO2 capture in a global scenario: consequences and alternatives, Desalination 380 (2016) 93–99, https://doi.org/10.1016/j.desal. 2015.08.004.

[92] L. Faramarzi, G.M. Kontogeorgis, M.L. Michelsen, K. Thomsen, E.H. Stenby, Absorber model for CO_2 capture by monoethanolamine, Ind. Eng. Chem. Res. 49 (8) (2010) 3751–3759, https://doi.org/10.1021/ie901671f.

[93] B.-H. Li, N. Zhang, R. Smith, Simulation and analysis of CO2 capture process with aqueous monoethanolamine solution, Appl. Energy 161 (2016) 707–717, https://doi.org/10.1016/j.apenergy.2015.07.010.

[94] H.-B. Xie, J. Elm, R. Halonen, N. Myllys, T. Kurtén, M. Kulmala, H. Vehkamäki, Atmospheric fate of monoethanolamine: enhancing new particle formation of sulfuric acid as an important removal process, Environ. Sci. Technol. 51 (2017) 8422–8431, https://doi.org/10.1021/acs.est.7b02294.

[95] J. Shen, H.-B. Xie, J. Elm, F. Ma, J. Chen, H. Vehkamäki, Methanesulfonic acid-driven new particle formation enhanced by monoethanolamine: a computational study, Environ. Sci. Technol. 53 (24) (2019) 14387–14397, https://doi.org/10.1021/acs.est.9b05306.

[96] M. Engsvang, H. Wu, Y. Knattrup, J. Kubečka, A.B. Jensen, J. Elm, Quantum chemical modeling of atmospheric molecular clusters involving inorganic acids and methanesulfonic acid, Chem. Phys. Rev. 4 (2023) 031311, https://doi.org/10.1063/5.0152517.

[97] Y. Liu, H.-B. Xie, F. Ma, J. Chen, J. Elm, Amine-enhanced methanesulfonic acid-driven nucleation: predictive model and cluster formation mechanism, Environ. Sci. Technol. 56 (2022) 7751–7760, https://doi.org/10.1021/acs.est.2c01639.

[98] R.D. Dennington, T.A. Keith, J.M. Millam. GaussView 5.0. 9; Gaussian Inc., Wallingford, CT, USA, 2008.

[99] M.J. Frisch, G.W. Trucks, H.B. Schlegel, G.E. Scuseria, M.A. Robb, J.R. Cheeseman, G. Scalmani, V. Barone, G.A. Petersson, H. Nakatsuji et al. Gaussian 16, Rev. C.01, Gaussian, Inc.: Wallingford, CT, USA, 2016.
[100] Y. Zhao, D.G. Truhlar, The M06 suite of density functionals for main group thermochemistry, thermochemical kinetics, noncovalent interactions, excited states, and transition elements: two new functionals and systematic testing of four M06-class functionals and 12 other functionals, Theor. Chem. Acc. 120 (2008) 215–241, https://doi.org/10.1007/s00214-007-0310-x.
[101] J. Chai, M. Head-Gordon, Long-range corrected hybrid density functionals with damped atom-atom dispersion corrections, Phys. Chem. Chem. Phys. 10 (2008) 6615–6620, https://doi.org/10.1039/B810189B.
[102] J. Chai, M. Head-Gordon, Systematic optimization of long-range corrected hybrid density functionals, J. Chem. Phys. 128 (2008) 084106, https://doi.org/10.1063/1.2834918.
[103] J. Elm, M. Bilde, K.V. Mikkelsen, Assessment of density functional theory in predicting structures and free energies of reaction of atmospheric prenucleation clusters, Chem. Theory Comput. 8 (2012) 2071–2077, https://doi.org/10.1021/ct300192p.
[104] E.D. Glendening, A.E. Reed, J.E. Carpenter, F. Weinhold, NBO Version 3.1.
[105] J.P. Foster, F. Weinhold, Natural hybrid orbitals, J. Am. Chem. Soc. 102 (1980) 7211–7218, https://doi.org/10.1021/ja00544a007.
[106] A.E. Reed, F. Weinhold, Natural bond orbital analysis of Near-Hartree-Fock water dimer, J. Chem. Phys. 78 (1983) 4066–4073, https://doi.org/10.1063/1.445134.
[107] L. Partanen, H. Vehkamäki, K. Hansen, J. Elm, H. Henschel, T. Kurtén, R. Halonen, E. Zapadinsky, Effect of conformers on free energies of atmospheric complexes, Chem. A Eur. J. 120 (2016) 8613–8624, https://doi.org/10.1021/acs.jpca.6b04452.
[108] J. Xu, B.J. Finlayson-Pitts, R.B. Gerber, Proton transfer in mixed clusters of methanesulfonic acid, methylamine, and oxalic acid: implications for atmospheric particle formation, Chem. A Eur. J. 121 (2017) 2377–2385, https://doi.org/10.1021/acs.jpca.7b01223.
[109] J.D. Dunitz, Organic fluorine: odd man out, ChemBioChem 5 (2004) 614–621, doi: 10.1002/cbic.200300801.
[110] J.D. Dunitz, R. Taylor, Organic fluorine hardly ever accepts hydrogen bonds, Chem. Eur. J. 3 (1997) 89–98, https://doi.org/10.1002/chem.19970030115.
[111] E.E. Fileti, R. Rivelino, S. Canuto, Rayleigh light scattering of hydrogen bonded clusters investigated by means of *ab initio* calculations, J. Phys. B Atomic Mol. Phys. 36 (2003) 399–408, https://doi.org/10.1088/0953-4075/36/2/319.
[112] P. Chaudhuri, S. Canuto, Rayleigh scattering properties of small polyglycine molecules, J. Mol. Struct. 760 (2006) 15–20, https://doi.org/10.1088/0953-4075/36/2/319.
[113] A.M. da Silva, S. Chakraborty, P. Chaudhuri, Rayleigh light scattering from hydrogen-bonded dimers of small astrophysical molecules, Int. J. Quantum Chem. 112 (2012) 2822–2827, https://doi.org/10.1002/qua.23303.
[114] J. Elm, P. Norman, M. Bilde, K.V. Mikkelsen, Computational study of the Rayleigh light scattering properties of atmospheric prenucleation clusters, PCCP 16 (2014) 10883–10890, https://doi.org/10.1039/C4CP01206B.